Structure–function relations of primate lower incisors: a study of the deformation of *Macaca mulatta* dentition using electronic speckle pattern interferometry (ESPI)

Netta Lev-Tov Chattah,[1]* Kornelius Kupczik,[2]* Ron Shahar,[3] Jean-Jacques Hublin[2] and Steve Weiner[1]

[1]*Department of Structural Biology, Weizmann Institute of Science, Rehovot, Israel*
[2]*Department of Human Evolution, Max Planck Institute for Evolutionary Anthropology, Leipzig, Germany*
[3]*Koret School of Veterinary Medicine, the Hebrew University of Jerusalem, Rehovot, Israel*

Abstract

Teeth adopt a variety of different morphologies, each of which is presumably optimized for performing specific functions during feeding. It is generally agreed that the enamel cap is a crucial element in controlling the mechanical behavior of mammalian teeth under load. Incisors are particularly interesting in terms of structure–function relations, as their role in feeding is that of the 'first bite'. However, little is known how incisor cap morphology is related to tooth deformation. In the present paper we examine the mechanical behavior of mandibular central incisors in the cercopithecine primate *Macaca mulatta* under loads similar to those encountered during ingestion. We map three-dimensional displacements on the labial surface of the crown as it is compressed, using electronic speckle pattern interferometry (ESPI), an optical metrology method. In addition, micro-computed tomography is used to obtain data regarding the morphology of the enamel cap, which in the *M. mulatta* lower incisors exhibits missing or very little enamel on the lingual face. The results showed that although compressed along a longitudinal axis, deformation in the incisors mostly occurred in the lingual direction and orthogonal to the direction of the applied load. Both isolated, embedded teeth and teeth in the mandible showed considerable lingual deformation. Incisor deformation in the mandible was generally greater, reflecting the additional freedom of movement enabled by the supporting structures. We show that the association with adjacent teeth in the arch is significant for the behavior of the tooth under load. Finally, loading two teeth simultaneously in the mandible showed that they work as one functional unit. We suggest that these results demonstrate the importance of enamel cap morphology in directing deformation behavior; an ability stemming from the stiffness of the enamel cap overlying the more pliable dentin.

Key words electronic speckle pattern interferometry; incisors; primate; structure–function.

Introduction

Vertebrate teeth and their supporting structures are adapted to dissipate forces incurred during feeding and are designed to maintain their functionality over prolonged periods of time (Lucas, 2007). Teeth adopt a variety of different morphologies, each of which is presumably optimized for performing specific functions during ingestion and mastication. Understanding the manner in which a whole tooth dissipates applied loads is complex. However, experimental studies and numerical simulations specifically emphasize the importance of the enamel cap in controlling the mechanical behavior of mammalian teeth under load (Yettram et al. 1976; Spears et al. 1993; Spears & Macho, 1998; Wang & Weiner, 1998; Magne et al. 1999; Palamara et al. 2000a,b; Wood et al. 2003; Zaslansky et al. 2006b; Lev-Tov Chattah et al. 2009; Barak et al. 2009). Incisors are particularly interesting in terms of structure–function relations, as their role in feeding is that of the 'first bite' (Agrawal et al. 2008; Lucas et al. 2008). Here we examine the mechanical behavior of mandibular incisors in the

rhesus macaque (*Macaca mulatta*) under loads and conditions similar to those encountered during ingestion, using an experimental approach.

Anthropoid primate incisor shape is spatulate and is usually approximated as a wedge in theoretical models (Ang et al. 2006; Agrawal et al. 2008). This spatulate shape is thought to have evolved in association with fruit eating (Agrawal et al. 2008 and references therein). Incisor function during ingestion mainly involves gripping and ⁄ or fracturing solids (Lucas, 2007; Lucas et al. 2008). Although this may seem like a simple process, incision is complex and relatively poorly understood. Much of the research on incisors has concentrated on primate incisor shape, size and enamel thickness in relation to diet (Hylander, 1975; Shellis & Hiiemae, 1986; Aimi & Nogami, 1989; Ungar, 1996, 1998; McCollum, 2007; Deane, 2009a,b). Larger incisors are thought to reflect consumption of tough, large items requiring fracture (for example fruits and bark), while smaller incisors are thought to reflect leaf consumption that requires mainly gripping (Hylander, 1975). However, this has been challenged as no straightforward relationship has been found between the degree of frugivory ⁄ folivory and incisor size alone in great apes (McCollum, 2007). More recently, Deane (2009a,b) has suggested that combining data regarding incisor size and incisor curvature (i.e. morphology) can be a more sensitive predictor of diet in hominoids. Enamel distribution on the incisors has also been associated with the degree of frugivory or folivory (Shellis & Hiiemae, 1986; Aimi & Nogami, 1989). Shellis & Hiiemae (1986) showed that frugivorous or omnivorous cercopithecines and papionins have little or no enamel on the lingual aspect of their lower incisors compared to the substantial enamel layer found in folivorous colobines. They suggest that thin enamel on the lingual aspect of the lower incisors creates a self-sharpening mechanism of the incisal edge, which is functionally important for fracturing tough foods and facilitates the consumption of a wider range of foodstuffs. Mandibular movement in this case is predominantly vertical. In contrast, the authors suggest that thicker enamel on the lingual aspect of the teeth, as found in colobines, creates a blunt incisal working surface which is more suited for gripping and tearing leaves, involving mainly a medio-lateral motion of the jaw.

The objective of this study is to understand the manner in which the mandibular incisors of *M. mulatta* deform during ingestion. Our strategy is to subject the incisors to compressive loads comparable in magnitude and direction to those incurred during ingestion. As incisor movement in *M. mulatta* is thought to be predominantly vertical (Shellis & Hiiemae, 1986), load is applied perpendicular to the longitudinal axis of the tooth. As the incisors are mechanically compressed, quantitative data is gathered on the displacements occurring on the labial surface of the crown using electronic speckle pattern interferometry (ESPI). ESPI is a non-contact, non-destructive optical metrology method,

and is used to produce high-resolution, full-field, three-dimensional surface deformation maps of the crown under load (Zaslansky et al. 2006b; Barak et al. 2009; Lev-Tov Chattah et al. 2009). A unique set-up allows teeth to be tested under water, ensuring that the *in vivo* biomechanical properties of dentin, enamel and bone, known to be altered by drying, are preserved (Rho & Pharr, 1999; Zaslansky et al. 2005). This approach has already been applied successfully to the study of whole-tooth mechanical behavior of minipig molars and human premolars (Zaslansky et al. 2006b; Barak et al. 2009; Lev-Tov Chattah et al. 2009); tooth types with enamel caps that cover the dentin core. In addition, micro-computed tomography (μCT) is used in the present study to obtain data regarding the macro-morphology of the enamel cap of the teeth under study.

Despite the thin or missing enamel on the lingual face of the lower incisors (Shellis & Hiiemae, 1986; Aimi & Nogami, 1989), we expect that crown deformation of *M. mulatta* incisors under load will be dominated by the morphology of the stiff enamel cap, as it does in teeth with both labial and lingual enamel. It has recently been shown that the full enamel cap of minipig molars deformed under axial compression by bending along the direction of the applied load, meaning that most of the deformation occurred along the longitudinal axis (Lev-Tov Chattah et al. 2009).

To study the mechanical behavior of the tooth crown as an isolated unit as well as the deformation behavior of the tooth crown when located within its supporting structures, the teeth were tested both in the mandible and after being extracted and embedded in a stiff polymer. A comparison between these two datasets can thus provide indirect data regarding the role of the supporting structures in dissipating stresses applied to the tooth (Asundi & Kishen, 2000, 2001).

Finally, in the mandible, the left and right central incisors were compressed individually (Fig. 1B) and then simultaneously (Fig. 1A). Compressing the central incisors in the mandible simultaneously simulates the manner in which they are loaded during incision, while compressing each incisor individually provides data regarding the manner in which adjacent teeth may affect the biomechanical behavior of a single tooth. Proper proximal contact areas are cru-
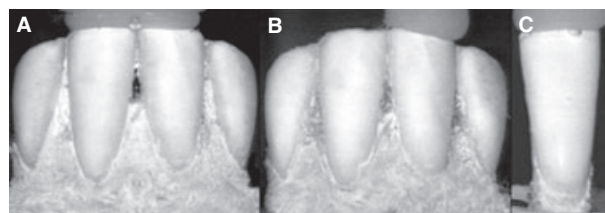

Fig. 1 Loading schemes for central incisors: (A) Both incisors loaded simultaneously while in the mandible; (B) Single incisor loaded while in the mandible; (C) Single incisor loaded after being extracted from the mandible and embedded in stiff polymer.

cial for normal function of the dentition (Kyoung-Hua et al. 2008); however, the affect of the proximal contact areas on the behavior of a tooth in short-term loading has not been studied.

Materials and methods

Dental samples

Fresh cadaveric heads of two adult male *M. mulatta* (DPZ 7845 and DPZ 7846; 8 and 9 years old, respectively) were obtained from the Deutsches Primatenzentrum (Göttingen, Germany). The heads were sterilized using gamma irradiation at 40 kGy (Gamma-Service Produktbestrahlung GmbH, Radeberg, Germany) and stored at −20 °C. After scanning the heads using a CT scanner (see below), the heads were dissected to remove the soft tissues, and the mandibles were detached.

The macaques were originally fed on a diet of fruits and vegetables as well as Old World monkey pellets. The proportion of fruit ⁄ vegetables to pellets was about two-thirds to three-thirds. The animals were kept in cages containing spruce branches for environmental enrichment. All permanent teeth were in occlusion. The dentin of the incisors was exposed in both specimens but there were no signs of carious lesions or chipped enamel.

Micro-computed tomography

The mandibles were scanned at 28 μm resolution with a BIR ACTIS 225 ⁄ 300 high-resolution industrial μCT scanner (Department of Human Evolution, Max Planck Institute for Evolutionary Anthropology, Leipzig). Image analysis was carried out using AVIZO 5.1.2 software (Mercury Computer Systems). In addition, images of isolated tooth crowns were obtained by μCT scanning at 16 μm resolution using the GE Healthcare eXplore Locus SP μCT instrument (Weizmann Institute of Science, Rehovot, Israel). Evaluation of the scanned volumes was carried out using GE Healthcare EXPLORE MICROVIEW v. 2.0 3D volume viewer software.

ESPI loading set-up and sample preparation

For the in-the-mandible configuration, the mandible was sectioned on either side of the lateral incisor (I_2) without compromising the integrity of the bone immediately surrounding the root of the tooth. Cutting the section distally to the I_2 maintains the *in vivo* restriction of the central incisor (I_1) in the dental arch (Fig. 1A,B). The sections were kept frozen at −20 °C until testing. A previous study noted that freezing had an impact on displacement magnitudes of minipig molars loaded in this configuration, i.e. frozen samples showed greater displacement magnitudes compared to fresh samples (Lev-Tov Chattah et al. 2009).

The teeth were first coated with a thin coat of white waterproof spray. This is a common procedure in optical testing intended to increase the light intensity reflected from the sample (Yang et al. 2007). To allow mounting, the segment was put in a round hollow depression within a stainless-steel ball-bearing and embedded in self-cure dental acrylic resin (JET acrylic, Lang Dental, IL; flexure modulus ∼3 GPa). Only the lower two-

thirds of the mandible was embedded, leaving the cervical third of the mandible, as well as the teeth, exposed (Fig. 1A,B). The ball-bearing enabled the alignment of each segment along a longitudinal orientation to mimic, to some extent, *in vivo* loading conditions. After testing, the section was extracted from its holder and the tooth was carefully removed from the boney socket. The isolated tooth was then embedded in acrylic up to a level just beneath the cement-enamel junction (Fig. 1C). Special efforts were made to keep the tooth and bone hydrated during these processes.

For the in-the-mandible configurations, each central incisor was compressed individually and both central incisors were compressed together. For the isolated tooth configuration each crown was loaded separately (Fig. 1C). The loading procedure was similar for both the in-the-mandible and isolated configurations, as follows. The specimen embedded in the metal ball-bearing was securely mounted in the testing chamber and aligned along a longitudinal or axial orientation (as in Fig. 2A). The flat surface of the upper mobile anvil was coated with a small amount of dental composite (Z100, 3M-ESPE, flexure modulus 14.5 GPa), which was then cured by light for 60 s (LITEX 682, Dentamerica, San Jose, CA). Another small amount of dental composite was placed on top of the previously cured layer and the anvil was lowered such that the uncured composite came in contact with and flowed over the incisal edge of the tooth, partially enveloping it (Fig. 1). The dental composite was again cured and the anvil was lowered further until a pre-load compression of ∼7 N was obtained. Finally, the test chamber was sealed with a high-grade glass window (BK-7 *l*/10 grade) and filled with water. Detailed information regarding the computer-controlled loading device is presented in Zaslansky et al. (2005). Each tooth was incrementally loaded in the Y direction along the longitudinal axis of the crown by the upper anvil using 2-μm increments. Teeth in-the-mandible were loaded to a total of 100 μm (50 steps) and isolated teeth were loaded to a total of 82 μm (41 steps). A 1.5-s pause is required for ESPI measurements between successive increments. The data thus provide discrete deformation maps for each loading increment. After each loading sequence the anvil returned to its pre-load position. The loading sequence was repeated four times with a 5-min interval between each compression set. After completing the part of the experiment in which one tooth was loaded, the anvil was raised and the chamber was opened. The hardened
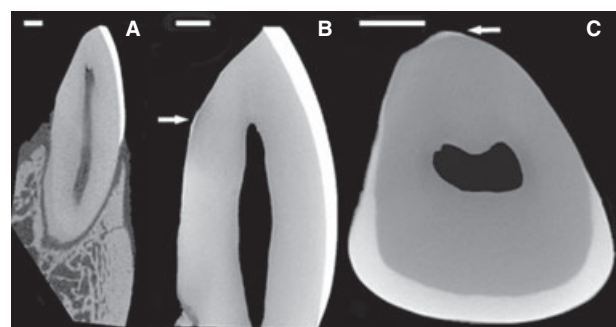

Fig. 2 Micro-CT of the central incisors: (A) Axial view of the incisor in the bone; (B) Close-up of the axial view of the extracted incisor; note the thin and scant enamel on the lingual aspect of the tooth as indicated by the arrow; (C) Transverse view of the extracted incisor. Scale bar: 1 mm.

composite was removed and fresh composite was reapplied on the adjacent tooth without changing the set-up. The chamber was sealed, filled with water, and four loading sequences were carried out. By repeating the loading sequence, a robust and repeatable dataset is obtained.

ESPI optical measurements and data analysis

The ESPI technique used in this study has been described previously in detail (Zaslansky et al. 2005). Briefly, an ESPI device (Q300; Dantec–Ettemeyer, Ulm, Germany), was used to record surface displacements on the labial side of the incisors as they were loaded. The surface of the tooth was illuminated by a coherent laser light source (780 nm wavelength). As coherent laser light scatters from the optically rough surface of the tooth, speckles are formed due to local interference and are imaged onto a CCD detector array. The difference between patterns of consecutive speckle images taken before and after applying the load are used to detect shifts in the phases of the speckles. These phase shifts correspond to displacements of the surface along the measurement axis and their extent can be determined using a phase-shifting algorithm combined with phase unwrapping. It is therefore possible to measure displacements as small as 25 nm along three orthogonal axes (X, Y, and Z) and generate displacement maps relative to an arbitrarily selected reference point located within a defined region of interest (ROI). The location of the reference point in this set of experiments was selected to be in the middle of the base of the ROI, where absolute displacements (relative to an external system) of the cervical part of the enamel cap are assumed to be the lowest for all three axes. ESPI measurements are insensitive to whole body translation, but do detect with great sensitivity deformations and rotations. For this study, displacement maps were generated by finding the cumulative displacement of each pixel for the entire set of incremental anvil movements and then averaging the cumulative maps of all four repeats. To standardize the results, data analyses were truncated at loads of ~80 N, the highest common cumulative force reached for all teeth. Mean maximal bite force in adult male *M. mulatta* incisors has been calculated at ~139 N (Dechow & Carlson, 1990).

Results

Micro-computed tomography

A μCT image of an incisor in the mandible (Fig. 2A) shows that the crown and root of the central incisor are approximately of equal height. In general the cross-sectional tooth is oval-shaped with relatively smooth surfaces. The cortical bone thickness is asymmetric, with the labial cortical bone having greater thickness than the lingual cortical bone. The periodontal ligament (PDL) space is also asymmetric, showing greater thickness at the root apex and cervical area.

Higher resolution images of the right central incisor crowns clearly show the relatively thick labial enamel which curves lingually (towards the oral cavity). While a thin enamel layer was found on the lingual face of one tooth (Figs. 2B,C), enamel was not detected on the lingual face of

Fig. 3 Micro-CT isosurface of the incisor enamel cap. Scale bar: 1mm.

the other tooth (Fig. 2A). This is consistent with previous reports (Shellis & Hiiemae, 1986; Aimi & Nogami, 1989) which showed that all cercopithecines have little or no enamel on the lingual aspect of their lower incisors. Figure 3 illustrates the shape of the enamel cap from the proximal aspect (side view) and shows that enamel in the incisal edge of the crown 'wraps' around the sides of the tooth, but is not present in the middle and cervical parts of the crown. The enamel cap may be described as incomplete, dominated by a lingually curved elongated plate on its labial face.

Tooth deformation

Figures 4 and 5 show displacement maps in the X, Y, and Z directions at ~80 N load. Figure 4 represents the tooth-in-mandible set-up and Fig. 5 the isolated, embedded teeth. Average displacement magnitudes of defined regions are provided along with the displacement direction that occurred in the averaged region. Teeth loaded individually in the mandible show varying displacement magnitudes, but similar trends in each displacement direction. Despite being loaded in the Y direction, the largest deformations occur in the Z or 'out-of-plane' direction, followed by the X direction. Deformation in the loading (Y) direction was minimal.

Deformation behaviors were similar between teeth. In the X direction each individual tooth is deformed distally (i.e. away from the midline of the mandible), and in the Y direction the incisal edge moved slightly up, whereas the
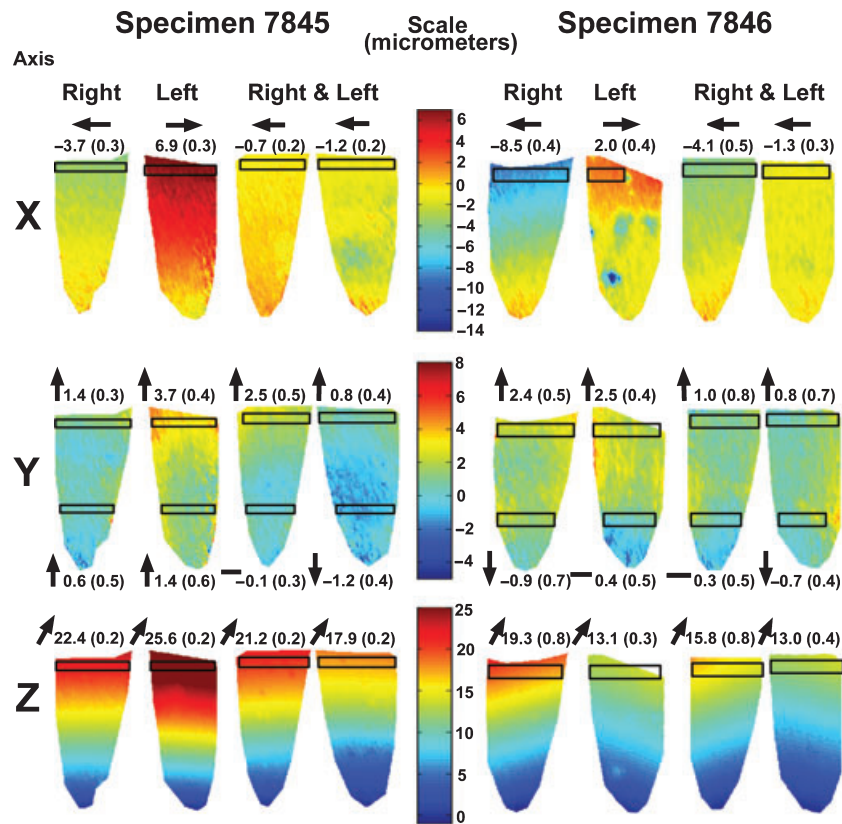
Fig. 4 Displacement maps of the incisors in the mandible: The maps show displacement which occurred on the surface of the enamel in each of the four teeth examined, at 80N load in the X, Y and Z directions. The color-code (micrometers) is presented separately for each direction. For each specimen the two left columns represent teeth loaded individually and the two right columns represent the two teeth loaded simultaneously. Transparent boxes represent areas where the displacements were averaged. The average displacement in these regions (in micrometers) as well as the direction of movement (as indicated by arrows) is presented respectively.

middle-cervical portion was barely displaced. The apparent displacement of the incisal edge away from the reference point is due to lingual bending (towards the oral cavity) in the Z direction.

When loaded simultaneously, both pairs of teeth showed overall decreased magnitudes of deformation. Nevertheless, similar displacement magnitude trends observed for individual teeth were also observed in this loading configuration. Deformation behavior showed that in the X direction the left crown was displaced mesially (i.e. towards the midline), whereas the right crown was displaced distally (i.e. away from the midline). The teeth were therefore displaced in unison (Fig. 4). In the Y and Z directions the displacement trends were similar to those found when the teeth were loaded individually.

Displacement magnitudes were generally lower in the teeth embedded in stiff polymer compared to teeth in the mandible that were loaded individually. However, the displacement magnitudes were comparable to teeth in the mandible loaded together. Deformation direction trends noted for teeth in the mandible were maintained, with the Z direction showing considerable deformation, followed by

the X direction. Very little deformation occurred in the Y direction.

Deformation behavior in the isolated embedded teeth differed from the deformation behavior of the teeth in the mandible, both in the X and Y directions, but was similar in the Z direction. In the X direction both left and right teeth were deformed mesially towards the midline. Although little movement occurs in the Y direction, an observed deformation gradient shows that the distal flanks of the tooth were deformed upwards, whereas the mesial flanks were displaced downwards. Combined with the movement in the X direction and the lingual displacement in the Z direction, this represents a three-dimensional bending motion of the tooth crown mesio-lingually.

Discussion

The aim of the present study is to understand the deformation behavior of *M. mulatta* central lower incisors under load conditions similar to those encountered during ingestion. We demonstrated that under vertical loads, the enamel mainly bends lingually in the Z 'out-of-plane'
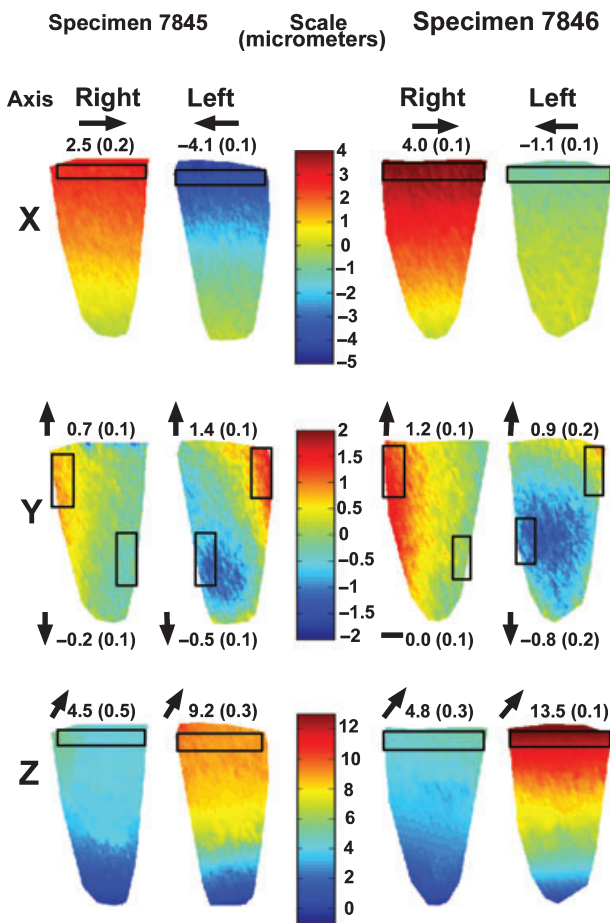
Fig. 5 Displacement maps of the incisors in stiff polymer: The maps show displacement which occurred on the surface of the enamel in each of the four teeth examined, at 80N load in the X, Y and Z directions. The color-code (micrometers) is presented separately for each direction. Transparent boxes represent areas where the displacements were averaged. The average displacement in these regions (in micrometers) as well as the direction of movement (as indicated by arrows) is presented respectively.

direction, orthogonal to the applied load direction. Overall, deformation magnitudes were greater for incisors in the mandible compared to those embedded in stiff polymer. However, considerable deformation was recorded in the isolated embedded teeth, particularly in the 'out-of-plane' direction. When compressed individually in the mandible, the central incisors deformed slightly away from the midline. When the same teeth were isolated and embedded they deformed by bending towards the midline. Finally, teeth in the mandible compressed together, deformed in unison.

Several factors act together to determine the behavior of the tooth as stress is applied to the crown, namely tooth crown morphology and structure, the supporting structures (i.e. socket geometry, PDL, alveolar bone) and the association of the tooth under load with adjacent teeth in the

dental arch. Each of these parameters will be discussed separately.

Incisor crown morphology

The *M. mulatta* central incisor as a whole is an elongated structure with a roughly oval cross-section (Fig. 1A,B). μCT data showed that the enamel cap of the *M. mulatta* lower central incisors examined is curved lingually and only partially covers the dentin core (Figs 2C and 3). In fact, as has been previously described elsewhere and reiterated here, in cercopithecines and papionins the enamel is confined to the labial surface of the lower incisor crown with some vestigial lingual enamel occasionally present (Shellis & Hiiemae, 1986; Aimi & Nogami, 1989). Thus the enamel layer for the most part resembles a thick lingually curved plate with thin edges wrapping around the dentin core. This gouge-shaped configuration enables the incisor to maintain a sharp incisal edge adapted to the reduction of tough food objects such as fruit rinds and bark (Walker, 1976; Shellis & Hiiemae, 1986). Such a structure will thus bend lingually under an axially applied force, provided the dentin and/or the supporting structures are comparably less stiff than the enamel. In contrast, a hypothetical body of a similar shape composed of a single isotropic material and loaded along its longitudinal axis would be expected to deform most in the loading direction (i.e. in the Y direction). Indeed, as we have observed here, in both the isolated, embedded teeth and the teeth in the mandible most of the deformation occurred lingually in the 'out-of-plane' direction and not in the loading direction along the long axis of the tooth. Deformation of the crown in a labio-lingual plane is supported by data which shows that in cercopithecines as opposed to colobines, wear striations on the incisors are oriented labio-lingually (Walker, 1976). The results of our study underline the crucial role played by the enamel cap in dictating whole crown behavior under load and can be attributed to the high elastic modulus of enamel compared to that of dentin (for human incisors see: Fong et al. 2000). In human incisors, the average elastic modulus of enamel ranges between 96 and 98 GPa, whereas dentin has a value of 25 GPa (Fong et al. 2000). In human molars, for example, the elastic modulus of enamel is approximately 115 GPa at the crown surface, gradually decreasing to 70 GPa at the interface with the dentin (Cuy et al. 2002). Bulk dentin is graded as well, with modulus values ranging between 15 and 30 GPa (Kinney et al. 1996, 1999, 2003). Moreover, studies have indicated that the functional width of the dentin at the dentin-enamel junction is much wider than the 5–30-μm-thick mantle dentin (Linde & Goldberg, 1993). The mantle dentin is a layer just underneath the enamel organ which is structurally and chemically different from bulk dentin (Linde & Goldberg, 1993). The functional dentin at the dentin-enamel junction is an approximately 200–300-μm-wide region whose stiffness is lower than that of bulk

dentin (Wang & Weiner, 1998; Tesch et al. 2001; Zaslansky et al. 2006a). Such a 'soft zone' has been identified in human premolars and in minipig molars (Zaslansky et al. 2006a; Lev-Tov Chattah et al. 2009), and is believed to serve as a stress-dissipating mechanism. Wood et al. (2003) used Moiré interferometry to examine deformation of tooth sections under changing humidity conditions. They measured tooth slices in which the enamel was present as a continuous ring around the dentin and slices where the dentin was only partially constricted. The latter configuration is to some extent analogous to the partial enamel covering of the dentin core in the *M. mulatta* incisor. Their results showed that in the constricted samples, little deformation occurred in the dentin, implying that the enamel ring constrained the tendency of the dentin to expand or contract. Unconstricted slices showed large deformations in the dentin at the dentin-enamel interface. The study highlights the importance of the enamel cap in distributing stresses applied to the tooth, as well as the importance of the 'soft zone' in taking up strain in cases where the enamel cap does not constrain the dentin. The existence, structure and distribution of such a 'soft zone' in *M. mulatta* teeth has yet to be demonstrated and its role in stress distribution may differ from that observed in the robust and complete enamel caps of human premolars and minipig molars.

Tooth supporting structures

When the tooth is loaded in the alveolar bone socket, the behavior of the crown also indirectly reflects the geometry of the socket, the properties of the PDL and the bone. μCT images of an incisor in the socket show that the PDL space around the root is asymmetric (Fig. 2A). A marked asymmetry was also noted between the labial and lingual portions of the mandibular bone (Fig. 2A); the labial portion of the mandible is more massive and dominated by a thick cortical bone plate. This asymmetry is well known in anthropoids, but its function is still debated (Daegling & Hotzman, 2003).

The supporting structures of the tooth play a major role in dissipating stresses applied to the tooth crown (Asundi & Kishen, 2000, 2001 and references therein). In the present study their collective role is reflected in the greater deformations measured when the teeth were in the mandible as compared to isolated, embedded teeth. A similar effect was seen in minipig molars and was associated with a greater freedom to rotate in the socket (Lev-Tov Chattah et al. 2009).

The role of adjacent teeth in the dental arch

Tooth function in relation to other teeth, and loss of contact areas with adjacent teeth may be detrimental to the tooth and its supporting structures in the long-run (Kyoung-Hwa et al. 2008). One of the main functions of the contact areas between teeth in the arch is stabilization.

Over the long-term these areas increase in size due to a combination of wear and mesial drift (Begg, 1954; Scheid & Woelfel, 2007). To date, however, no study has examined the effect of adjacent teeth on the deformation behavior of a single tooth under short-term, real-time loading, as was done in our experiments. One of the advantages of our experimental set-up was that the anterior portion of the dental arch was left intact. Central incisor crowns in the mandible, loaded individually, were deformed differently in the X and Y directions compared to the isolated teeth embedded in stiff polymer (Figs 4 and 5). We suggest that this is mainly due to the constricting effect of the adjacent teeth. The fact that deformation behavior in the 'out-of-plane' direction remained the same in both configurations, serves to support this notion. This is also supported by a previous study that showed that when adjacent teeth were removed from the mandible, molars compressed in the mandible displayed identical deformation patterns as those embedded in a stiff polymer (Lev-Tov Chattah et al. 2009).

Finally, central incisors loaded simultaneously deformed in unison. This behavior is different from that observed for teeth loaded individually in the mandible as well as for isolated, embedded teeth. Deforming in unison is functionally advantageous as it allows the effective utilization of a wider working surface.

Conclusions

In this study we examined the deformation behavior of *M. mulatta* lower central incisors under load directions and magnitudes comparable to those encountered during ingestion. We confirmed that the *M. mulatta* lower incisors have very little enamel on their lingual face. When compressed along the longitudinal axis, deformation was predominantly in the lingual direction and orthogonal to the direction of the applied load. We suggest that this reflects the importance of the enamel cap morphology in cercopithecines in directing deformation behavior. This ability largely stems from the greater stiffness of the enamel cap overlaying the relatively more pliable dentin. In future studies we propose to examine experimentally and numerically the deformation behavior of colobine incisors with distinct enamel cap morphology compared to that of cercopithecines. This will enable the comparison of deformation behaviors in incisors adapted to very different ingestion modes, and may shed light on the adaptive significance of some of the biomechanical behaviors observed.

Acknowledgements

References

Agrawal KR, Ang KY, Sui Z, et al. (2008) Methods of ingestion and incisal designs. In: *Technique and Application in Dental Anthropology* (eds Irish JD, Nelson GC), pp. 349–363. Cambridge: Cambridge University Press.

Aimi M, Nogami Y (1989) *Macaca fuscata* develops thin enamel on lingual sides of lower incisors. *Primates* **30**, 261–262.

Ang KY, Lucas PW, Tan HTW (2006) Incisal orientation and biting efficiency. *J Hum Evol* **50**, 663–672.

Asundi A, Kishen A (2000) A strain gauge and photoelastic analysis of in vivo strain and in vitro stress distribution in human dental supporting structures. *Arch Oral Biol* **45**, 543–550.

Asundi A, Kishen A (2001) Advanced digital photoelastic investigations on the tooth-bone interface. *J Biomed Opt* **6**, 224–230.

Barak MM, Geiger S, Lev-Tov Chattah N, et al. (2009) Enamel dictates whole tooth deformation: a finite element model study validated by a metrology method. *J Struct Biol*, **168**, 511–520.

Begg PR (1954) Stone age man's dentition. *Am J Orthod* **40**, 298–312.

Cuy JL, Mann AB, Livi KJ, et al. (2002) Nanoindentation mapping of the mechanical properties of human molar tooth enamel. *Arch Oral Biol* **47**, 281–291.

Daegling DJ, Hotzman JL (2003) Functional significance of cortical bone distribution in anthropoid mandibles: an in vitro assessment of bone strain under combined loads. *Am J Phys Anthropol* **122**, 38–50.

Deane AS (2009a) First contact: understanding the relationship between hominoid incisor curvature and diet. *J Hum Evol* **56**, 263–274.

Deane AS (2009b) Early Miocene catarrhine dietary behaviour: the influence of the Red Queen Effect on incisor shape and curvature. *J Hum Evol* **56**, 275–285.

Dechow PC, Carlson DS (1990) Occlusal force and craniofacial biomechanics during growth in rhesus monkeys. *Am J Phys Anthropol* **83**, 219–237.

Fong H, Sarikaya M, White SN, et al. (2000) Nano-mechanical properties profiles across dentin-enamel junction of human incisor teeth. *Mater Sci Eng C* **7**, 119–128.

Hylander WL (1975) Incisor size and diet in anthropoids with special reference to Cercopithecidae. *Science* **189**, 1095–1098.

Kinney JH, Balooch M, Marshall SJ, et al. (1996) Hardness and Young's modulus of human peritubular and intertubular dentine. *Arch Oral Biol* **41**, 9–13.

Kinney JH, Balooch M, Marshall GW, et al. (1999) A micromechanics model of the elastic properties of human dentine. *Arch Oral Biol* **44**, 813–822.

Kinney JH, Marshall SJ, Marshall GW (2003) The mechanical properties of human dentin: a critical review and re-evaluation of the dental literature. *Crit Rev Oral Biol Med* **14**, 13–29.

Kishen A, Tan KB, Asundi A (2006) Digital moire interferometric investigations on the deformation gradients of enamel and dentine: an insight into noncarious cervical lesions. *J Dent* **34**, 12–18.

Kyoung-Hwa K, Jae-Hyun J, Hee-Jung K, et al. (2008) Evaluation of tightness of proximal contacts in permanent dentition. *J Korean Acad Prosthodont* **46**, 553–560.

Lev-Tov Chattah N, Shahar R, Weiner S (2009) Design strategy of minipig molars using electronic speckle pattern interferometry: comparison of deformation under load between the tooth-mandible complex and the isolated tooth. *Adv Mater* **21**, 413–418.

Linde A, Goldberg M (1993) Dentinogenesis. *Crit Rev Oral Biol Med* **4**, 679–728.

Lucas PW (2007) *Dental Functional Morphology: How Teeth Work*. New York: Cambridge University Press.

Lucas PW, Constantino PJ, Wood BA (2008) Inferences regarding the diet of extinct hominins: structural and functional trends in dental and mandibular morphology within the hominin clade. *J Anat* **212**, 486–500.

Magne P, Versluis A, Douglas WH (1999) Rationalization of incisor shape: experimental-numerical analysis. *J Prosthet Dent* **81**, 345–355.

McCollum MA (2007) Rethinking incisor size and diet in anthropoids: diet, incisor wear and incisor breadth in the African apes. *Am J Phys Anthropol* **133**, 986–993.

Palamara D, Palamara JE, Tyas MJ, et al. (2000a) Strain patterns in cervical enamel of teeth subjected to occlusal loading. *Dent Mater* **16**, 412–419.

Palamara JE, Palamara D, Messer HH (2000b) Strains in the marginal ridge during occlusal loading. *Aust Dent J* **47**, 218–222.

Rho JY, Pharr GM (1999) Effects of drying on the mechanical properties of bovine femur measured by nanoindentation. *J Mater Sci Mater Med* **10**, 485–488.

Scheid RC, Woelfel JB (2007) *Woelfel's Dental Anatomy: Its Relevance to Dentistry*. Baltimore: Lippincott Williams & Wilkins.

Shellis RP, Hiiemae KM (1986) Distribution of enamel on the incisors of Old World monkeys. *Am J Phys Anthropol* **71**, 103–113.

Spears IR, Macho GA (1998) Biomechanical behavior of modern human molars: implications for interpreting the fossil record. *Am J Phys Anthropol* **106**, 467–482.

Spears IR, van Noort R, Crompton RH, et al. (1993) The effects of enamel anisotropy on the distribution of stress in a tooth. *J Dent Res* **72**, 1526–1531.

Tesch W, Eidelman N, Roschger P, et al. (2001) Graded microstructure and mechanical properties of human crown dentin. *Calcif Tissue Int* **69**, 147–157.

Ungar PS (1996) Relationship of incisor size to diet and anterior tooth use in sympatric Sumatran anthropoids. *Am J Primatol* **38**, 145–156.

Ungar PS (1998) Dental allometry, morphology and wear as evidence for diet in fossil primates. *Evol Anthropol* **6**, 205–217.

Walker PL (1976) Wear striations on the incisors of cercopithecid monkeys as an index of diet and habitat preference. *Am J Phys Anthropol* **45**, 299–308.

Wang RZ, Weiner S (1998) Strain-structure relations in human teeth using Moire fringes. *J Biomech* **31**, 135–141.

Wood JD, Wang RZ, Weiner S, et al. (2003) Mapping of tooth deformation caused by moisture change using Moiré interferometry. *Dent Mater* **19**, 159–166.

Yang L, Zhang P, Liu S, et al. (2007) Measurement of strain distributions in mouse femora with 3D-digital speckle pattern interferometry. *Opt Lasers Eng* **45**, 843–851.

Yettram AL, Wright KW, Pickard HM (1976) Finite element stress analysis of the crowns of normal and restored teeth. *J Dent Res* **55**, 1004–1011.

Zaslansky P, Currey JD, Friesem AA, et al. (2005) Phase shifting speckle interferometry for determination of strain and Young's modulus of mineralized biological materials: a study of tooth dentin compression in water. *J Biomed Opt* **10**, 024020.

Zaslansky P, Friesem AA, Weiner S (2006a) Structure and mechanical properties of the soft zone separating bulk dentin and enamel in crowns of human teeth: insight into tooth function. *J Struct Biol* **153**, 188–199.

Zaslansky P, Shahar R, Friesem AA, et al. (2006b) Relations between shape, materials properties, and function in biological materials using laser speckle interferometry: in situ tooth deformation. *Adv Funct Mater* **16**, 1925–1936.